

X-ray Diffraction Study of Spontaneous Strain in Fe-Pnictide Superconductor, NdFeAsO_{0.89}F_{0.11}

メタデータ	言語: eng 出版者: 公開日: 2017-10-03 キーワード (Ja): キーワード (En): 作成者: メールアドレス: 所属:
URL	http://hdl.handle.net/2297/30171

X-ray Diffraction Study of Spontaneous Strain in Fe-Pnictide Superconductor, $\text{NdFeAsO}_{0.89}\text{F}_{0.11}$

H. Fujishita^{1 a}, Y. Hayashi², M. Saito², H. Unno², H. Kaneko¹, H. Okamoto³, M. Ohashi⁴, Y. Kobayashi^{5,6}, and M. Sato^{5,6,7b}

¹ School of Mathematics and Physics, Kanazawa University, Kanazawa, 920-1192, Japan

² Division of Mathematical and Physical Sciences, Kanazawa University, Kanazawa 920-1192, Japan

³ School of Health Sciences, Kanazawa University, Kanazawa 920-0942, Japan

⁴ School of Environmental Design, Kanazawa University, Kanazawa 920-1192, Japan

⁵ Department of Physics, Nagoya University, Furo-cho, Chikusa-ku, Nagoya 464-8602, Japan

⁶ JST, TRIP, Nagoya University, Furo-cho, Chikusa-ku, Nagoya 464-8602, Japan

⁷ Toyota Physical and Chemical Research Institute, Nagakute, Aichi 480-1192, Japan

Received: date / Revised version: date

Abstract. The lattice parameters of a Nd 1111 Fe-pnictide superconductor, $\text{NdFeAsO}_{0.89}\text{F}_{0.11}$, were accurately measured using X-ray diffraction between 20 K and 280 K. A very small change in the lattice parameter could be detected in the superconducting phase. This change can be attributed to a spontaneous strain generated in the superconducting phase by the coupling between a superconducting order parameter and the strain. The present results are compared with the thermal expansion coefficients of $\text{Ba}(\text{Fe}_{1-x}\text{Co}_x)_2\text{As}_2$, in addition to the previous lattice parameter measurements of $\text{YBa}_2\text{Cu}_3\text{O}_{6.5}$, MgB_2 , $\text{La}_{1.85}\text{Sr}_{0.15}\text{CuO}_4$, and $\text{Ba}_{0.6}\text{K}_{0.4}\text{BiO}_3$.

PACS. 74.70.Xa Pnictides and chalcogenides – 61.05.cp X-ray diffraction – 65.40.De Thermal expansion; thermomechanical effects

1 Introduction

The structural changes in high-temperature superconductors have been studied extensively using high-resolution diffractometers since the discovery of the superconducting phase transition in $\text{La}_{2-x}\text{Sr}_x\text{CuO}_4$. Nevertheless, no significant anomalies have been detected in connection with the superconducting phase transition. However, the following changes in lattice parameters were successfully detected in 2002. The lattice parameters of orthorhombic $\text{YBa}_2\text{Cu}_3\text{O}_{6.5}$, which has a superconducting transition temperature T_c of 55 K, were accurately measured using high-angle double-crystal X-ray diffractometry, and a change in the orthorhombicity, $2(b-a)/(a+b) = \tan^{-1}(b/a) - \pi/4$, at T_c was clearly detected [1]. An anomaly in lattice parameter a of the hexagonal intermetallic superconductor MgB_2 was clearly observed using high-resolution pulsed neutron powder diffraction [2]: The a -axis thermal expansion became negative near its T_c of 39 K.

A change of volume in a superconducting phase was first discussed thermodynamically on the basis of Gibbs

free energy, and the following relation was obtained [3]:

$$V_n - V_s(0) \cong \mu_0 V_s H_c \left(\frac{\partial H_c}{\partial p} \right)_T,$$

where V_n and V_s are the volumes in the normal and superconducting phases, respectively. H_c , p , and T are the critical magnetic field, pressure, and temperature, respectively. Using experimentally obtained values on the right hand side of the above equation, $\Delta V/V$ was deduced to be 10^{-7} . In the case of Sn, this value was found to be in good agreement with the observed value [3, 4].

For Ta and Nb (and most of the other elemental superconductors), specimen lengths were observed to expand with the occurrence of superconductivity, but a contraction was observed in the case of V [5]. The electronic contribution to the volume expansion coefficient and its discontinuity at T_c , expected by the standard Ehrenfest equation, was discussed based on the BCS theory; satisfactory agreements were achieved with experimental data for Nb and some technical alloys [6]. The linear expansion coefficients of various high- T_c superconductors were also measured using capacitance dilatometers and analyzed using the Ehrenfest equation [7, 8].

A spontaneous strain, i.e., a secondary order parameter, is typically produced through the coupling between

^a e-mail: fujishit@staff.kanazawa-u.ac.jp

^b Present address: Research Center for Neutron Science and Technology, Comprehensive Research Organization for Science and Society, Shirane, Tokai-mura, Ibaraki 319-1195, Japan

the strain e and the primary order parameter Q or an atomic shift in structural phase transitions. It is similar to the case of ferromagnets. In ferromagnets, small spontaneous strains are produced (i.e., spontaneous magnetostriction), where the order parameter Q is spontaneous magnetization. The strain in invar alloys is known to be so large that the alloys show low thermal expansion in their ferromagnetic phases [9]. The free energy $G(Q, T)$ near the transition temperature T_c can be expressed in its simplest form as follows, using a Landau potential:

$$G(Q, T) = G_0(T) + \frac{1}{2}A(T - T_c)Q^2 + \frac{1}{4}BQ^4 + \frac{1}{2}C|e|^2 - D|e|Q^2,$$

where A , B , C , and D are temperature independent positive constants. This free energy can be applied in the temperature range near T_c , not because of the existence of the coupling and elastic terms but because of an insufficient expression of the terms that do not include the strain. In the case of structural phase transitions, however, a quantum expansion of the Landau potential is applicable at all temperatures below T_c [10]. From the equilibrium condition for the strain, we can obtain the relation between the strain and order parameter as follows:

$$|e| = (D/C)Q^2.$$

The primary order parameter Q is zero above T_c , whereas it is nonzero below T_c . Thus, a linear-quadratic relation between the spontaneous strain and order parameter is expected in this simplest case. Because this relation is derived only from the terms that include e in $G(Q, T)$, it is expected to hold at all temperatures below T_c .

We carried out precise lattice parameter measurements of a high-temperature superconductor, $\text{La}_{1.85}\text{Sr}_{0.15}\text{CuO}_4$ [11], and a well-studied typical conventional superconductor, $\text{Ba}_{0.6}\text{K}_{0.4}\text{BiO}_3$ [12], using a conventional X-ray powder diffractometer. We could detect very small changes in the lattice parameters in their superconducting phases. We showed that these changes could be explained as spontaneous strain caused by the coupling between the strain and an energy gap $\Delta(T)$, i.e., a BCS gap, on a Fermi surface. We also showed that the changes in the lattice parameters of MgB_2 and $\text{YBa}_2\text{Cu}_3\text{O}_{6.5}$ could be attributed to this coupling [11, 12], in contrast to the interpretations given by the discoverers of the anomalies.

Recently, Fe-pnictide systems were discovered as a new kind of high-temperature superconductor [13]. For these systems, the so-called S_{\pm} symmetry with different signs for the order parameters (Δ) between the disconnected Fermi surfaces around the Γ and M points was proposed [14, 15]. However, an S_{++} symmetry with no sign difference between the two Δ values has been reported from both the experimental and theoretical view-points [16–18].

In the present study, we performed precise lattice parameter measurements on a Nd 1111 Fe-pnictide superconductor, $\text{NdFeAsO}_{0.89}\text{F}_{0.11}$, to clarify whether such coupling between the strain and superconducting energy gap is commonly observed in this new group of superconductors.

2 Experimental details

Polycrystalline samples of $\text{NdFeAsO}_{0.89}\text{F}_{0.11}$ were prepared from initial mixtures of Nd, Nd_2O_3 , NdF_3 , and FeAs at nominal molar ratios. Details of these preparations were given in our previous papers [19, 20].

X-ray diffraction patterns were measured using a Rigaku X-ray diffractometer, RINT2500, with a graphite counter monochromator and an X-ray generator with a rotating Cu anode. The generator was operated at 50 kV and 300 mA. A powder sample was obtained by grinding the polycrystalline powder. A plate-like powder sample was mounted on a sample holder made of copper. The sample was fixed in a closed-cycle He gas refrigerator that was mounted on the diffractometer. The sample was cooled from room temperature to 20 K. Diffraction patterns were measured between 20° and 140° at a scanning speed of $2\theta = 0.4^\circ/\text{min}$. Data were collected at every $2\theta = 0.02^\circ$. Measurements were performed twice or three times at the same temperature between 21 K and 280 K. The measurement at 20 K was made only once because of the limited ability of the refrigerator.

To accurately determine the T_c of the sample, we measured the magnetization of the powder sample used in the X-ray experiment. This measurement was performed in a magnetic field of 5 Oe after field cooling using a superconducting quantum interference device (SQUID) magnetometer, Quantum Design SP5000.

To obtain accurate lattice parameters, we analyzed the patterns using the whole-powder-pattern fitting method without reference to a structural model [21, 22]. This method uses lattice parameters and Miller indices only as structure-related parameters. Thus, the analyzed results are not affected by a preferred orientation effect. The Miller indices were obtained based on space group $P4/nmm$ (No. 129) [23]. Very weak reflections were omitted during the calculations, with seventy indices finally used. The background levels were fitted using polynomial expressions through the analyses. A pseudo-Voigt function was applied to the profile of the X-ray powder diffraction peaks. Least-squares refinements were carried out to minimize the R-factor R_{wp} , which is defined as follows:

$$R_{wp} = \sqrt{\frac{\sum_i w_i (y_i - f_i)^2}{\sum_i w_i y_i^2}},$$

where y_i and f_i are the observed and calculated intensities, respectively, at the i -th step. These intensities contain the background intensities. The weight w_i was taken to be equal to $1/y_i$.

The phenomenological temperature dependences of lattice parameters a and c above T_c were studied using the computer program KaleidaGraph.

3 Results

The results of the profile fitting at 20 K are shown in Figure 1, as an example. The R-factors of this fit were

$R_{wp} = 9.6\%$, $R_p = 6.0\%$, and $R_e = 5.4\%$. The obtained values of lattice parameters a and c are delineated in Figures 2 and 3, respectively, as a function of the temperature along with the magnetization for comparison: The lattice parameters are averages of the parameters obtained at the same temperature. Their estimated standard deviations (esds) were obtained by appropriately dealing with the esds of independent measurements from a statistical viewpoint. The magnetization showed a negative value below 48 K, indicating a superconducting transition temperature T_c of 48 K. We have to estimate the high-temperature

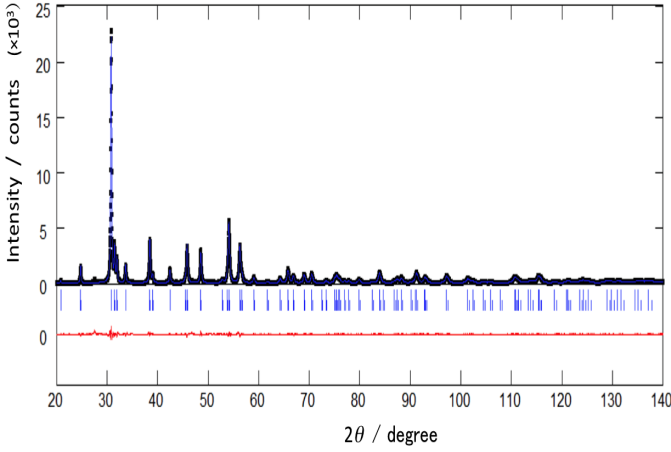


Fig. 1. X-ray powder diffraction pattern and best-fit refinement profile of $\text{NdFeAsO}_{0.89}\text{F}_{0.11}$ observed at 20 K. The calculated pattern is shown by a blue line passing through black data points in the upper portion. The short vertical blue bars below the pattern indicate the positions of the allowed reflections. The longer bars and shorter bars indicate those for $\text{CuK}\alpha_1$ and $\text{K}\alpha_2$ X-rays, respectively. The red line in the lower portion shows the differences between the observed and calculated patterns.

phase lattice parameters a_{HT} and c_{HT} by extrapolating to the same low temperature (i.e., the hypothetical lattice parameters of the high-temperature phase at a low temperature), because spontaneous strains e_a and e_c are originally defined as follows [24] and there are no approximate expressions in this case, in contrast to structural phase transitions:

$$\begin{aligned}
 e_a &= (a_{LT} - a_{HT})/a_{HT}, \\
 e_c &= (c_{LT} - c_{HT})/c_{HT},
 \end{aligned}$$

where a_{LT} and c_{LT} are low-temperature phase lattice parameters. To precisely estimate the a_{HT} and c_{HT} below T_c , we fitted a simple Einstein model to a and c above 48 K. The functions are expressed as

$$\begin{aligned}
 \ln(a/a_o) &= A_a \Theta_E^a [\exp(\Theta_E^a/T) - 1]^{-1}, \\
 \ln(c/c_o) &= A_c \Theta_E^c [\exp(\Theta_E^c/T) - 1]^{-1},
 \end{aligned}$$

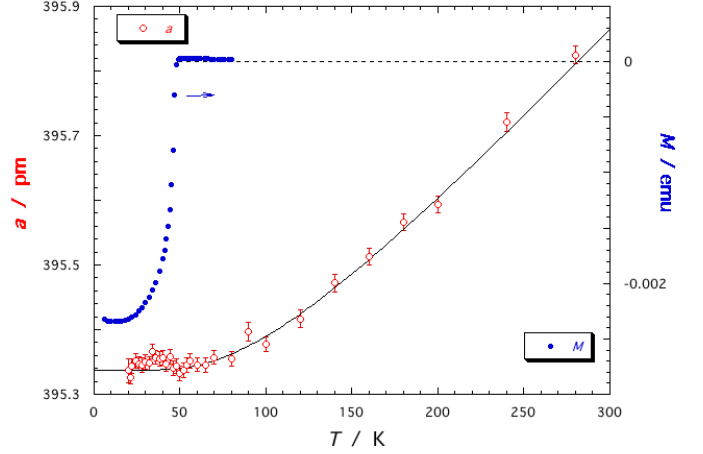


Fig. 2. Plots of lattice parameter a (red open circles: left-hand scale) and magnetization (blue solid circles: right-hand scale) of $\text{NdFeAsO}_{0.89}\text{F}_{0.11}$ versus temperature. The solid line shows the least-squares fit using a simple Einstein model to the data between T_c and 200 K and its extensions.

where a_o and c_o are the lattice parameters at $T = 0$, Θ_E^a and Θ_E^c are the Einstein temperatures, and A_a and A_c are the scaling coefficients, which include the Grüneisen parameters. A_a and A_c give the thermal expansion coefficients at high temperatures. The values of $(1/esd.)^2$ were used as the weights of the lattice parameters in the least-squares fittings.

Recently, the existence of structural modifications in $\text{NdFeAsO}_{0.85}$ was detected between a T_c of 53.5 K and ~ 180 K [25]. These modifications are accompanied by changes in the slopes of the temperature dependences of the lattice parameters at around ~ 180 K. Because we did not employ a dense temperature sampling on $\text{NdFeAsO}_{0.89}\text{F}_{0.11}$ above 200 K, we could not obtain clear changes in the slopes. However, preliminary analyses indicated that the c -axis lattice parameters at 240 K and 280 K deviated from an extension of the fitting for data below 200 K. Then, we applied the above equations to the data between T_c and 200 K for both the c -axis lattice parameters and the a -axis ones.

The results of the fitting to lattice parameter a and its extension below T_c are shown in Figure 2 by a solid line, where $\Theta_E^a = 278 \pm 44$ K, $A_a = (7.3 \pm 1.1) \times 10^{-6} \text{ K}^{-1}$, and the errors are the standard errors. The coefficient of determination, R^2 , of this fitting was 0.9945. The a_{HT} was almost temperature independent below T_c . No clear deviations of a_{LT} from a_{HT} could be detected in the superconducting phase. The results of the fitting to lattice parameter c and its extension below T_c are shown in Figure 3 by a solid line, where $\Theta_E^c = 195 \pm 12$ K, $A_c = (2.18 \pm 0.08) \times 10^{-5} \text{ K}^{-1}$, and $R^2 = 0.9997$. The function accurately reproduced the data above T_c until 200 K. The c_{HT} showed a slight temperature dependence below T_c until close to 30 K; the change below T_c was about 0.06 pm. The c_{LT} showed a very small negative thermal expansion, and a distinct deviation of c_{LT} from c_{HT} was observed in the super-

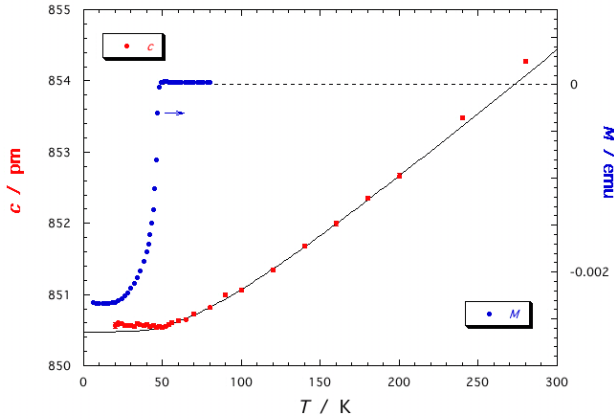


Fig. 3. Plots of lattice parameter c (red solid circles with error bars: left-hand scale) and magnetization (blue solid circles: right-hand scale) of $\text{NdFeAsO}_{0.89}\text{F}_{0.11}$ versus temperature. The solid line shows the least-squares fit using a simple Einstein model to the data between T_c and 200 K and its extensions.

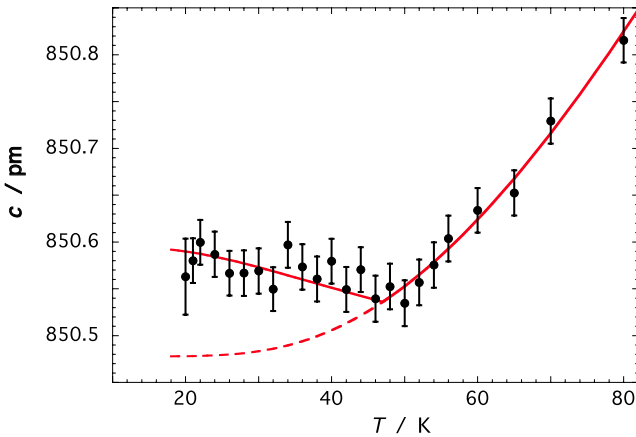


Fig. 4. Comparison between observed lattice parameter c (solid circles) and calculated one (solid line in superconducting phase) of $\text{NdFeAsO}_{0.89}\text{F}_{0.11}$. The solid line above T_c and the broken line below T_c are least-squares fits obtained using a simple Einstein model above T_c and its extension below T_c , respectively.

conducting phase. Figure 4 shows a comparison between the observed lattice parameter, c , and the calculated one (a red solid line) below 80 K. The red broken line indicates c_{HT} below T_c . The spontaneous strain, e_c , was obtained and compared with $\Delta^2(T)$. The numerical values of $\Delta(T)$ were taken from the table in ref. 26. The solid line below T_c in Figure 4 shows c_{LT} calculated for $e_c \propto \Delta^2(T)$; i.e., $c_{LT} = c_{HT} + c_{HT}K\Delta^2(T)$, where K is a proportional constant. The function accurately reproduced the data below T_c . Such a relationship is expected in the case of a linear-quadratic coupling between the strain and order parameter.

4 Discussion

We could detect a very small change in lattice parameter c of $\text{NdFeAsO}_{0.89}\text{F}_{0.11}$ below its superconducting transition temperature by X-ray diffraction. This change could be explained as a spontaneous strain caused by coupling with the superconducting order parameter. We previously obtained similar results for the high- T_c superconductor $\text{La}_{1.85}\text{Sr}_{0.15}\text{CuO}_4$ [11] and the well-studied conventional BCS superconductor $\text{Ba}_{0.6}\text{K}_{0.4}\text{BiO}_3$ [12]. An anomaly in lattice parameter a of the orthorhombic high- T_c superconductor $\text{YBa}_2\text{Cu}_3\text{O}_{6.5}$ with a T_c of 55 K was clearly observed at T_c [1]. A negative thermal expansion of a in the hexagonal intermetallic superconductor MgB_2 was clearly observed near its T_c of 39 K [2]. MgB_2 is now known to be a BCS superconductor showing two-band superconductivity [27]. We suggested that these published data could be satisfactorily explained in terms of the coupling [11, 12]. Thus, the lattice parameter anomalies observed in $\text{YBa}_2\text{Cu}_3\text{O}_{6.5}$, MgB_2 , $\text{La}_{1.85}\text{Sr}_{0.15}\text{CuO}_4$, $\text{Ba}_{0.6}\text{K}_{0.4}\text{BiO}_3$, and $\text{NdFeAsO}_{0.89}\text{F}_{0.11}$ could be explained as spontaneous strains caused by coupling with the superconducting order parameter.

As already mentioned in §3, structural modifications exist in $\text{NdFeAsO}_{0.85}$ [25]. These modifications appear between $T_{onset} \sim 180$ K and T_c of 53.5 K. The slopes of the temperature dependences of the a - and c -axis lattice parameters change between T_{onset} and $T_f \sim 135$ K. At around T_f , a modification in the temperature dependence is evidenced for several bond length characteristics. The c -axis lattice parameters of $\text{NdFeAsO}_{0.89}\text{F}_{0.11}$ at 240 K and 280 K deviated from an extended line of the least squares fit to the data between 200 K and a T_c of 48 K. These deviations might indicate that the structural modifications also exist in $\text{NdFeAsO}_{0.89}\text{F}_{0.11}$. The a -axis and c -axis lattice parameters of $\text{NdFeAsO}_{0.89}\text{F}_{0.11}$ at 90 K deviated slightly from the lines of the fittings, which might correspond to the T_f . A structural study with dense temperature sampling is desirable to clarify the existence of the structural modifications in $\text{NdFeAsO}_{0.89}\text{F}_{0.11}$. The temperature dependence of the c -axis, however, did not show an anomaly in $\text{NdFeAsO}_{0.85}$ below T_c , in contrast to the present result for $\text{NdFeAsO}_{0.89}\text{F}_{0.11}$. The anomaly below T_c in $\text{NdFeAsO}_{0.85}$ might be covered or repaired by the modifications.

In the x - T phase diagram for the $\text{Ba}(\text{Fe}_{1-x}\text{Co}_x)_2\text{As}_2$ system, superconductivity is observed between $x \sim 0.035$ and $x \sim 0.18$. Structural-antiferromagnetic phase transitions appear in their normal states below $x \sim 0.06$, while the phase transitions vanish above $x \sim 0.06$ [28, 29]. Precise thermal expansion measurements have been carried out on the system [30, 31]. To compare the present X-ray diffraction measurement results with these results, we calculated the coefficients based on the solid lines in Figures 2 and 3 above 48 K, along with the solid line in Figure 4 below 48 K. The temperature dependences of the coefficients are delineated in Figure 5. The values and temperature dependences of the coefficients above T_c are very similar to those of $\text{Ba}(\text{Fe}_{0.926}\text{Co}_{0.074})_2\text{As}_2$ [30] and $\text{Ba}(\text{Fe}_{0.92}\text{Co}_{0.08})_2\text{As}_2$ [31]. The coefficient along the a -axis showed a rapid change

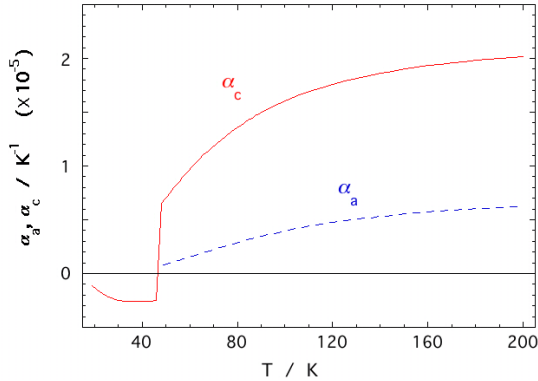


Fig. 5. Thermal expansion coefficients of $\text{NdFeAsO}_{0.89}\text{F}_{0.11}$. The lines above T_c were obtained by differentiating the fitted lines in Figures 2 and 3, while the α_c values below T_c were obtained by differentiating the fitted line in Figure 4. No α_a values below T_c could be obtained.

from almost zero to a positive value at T_c , after which it again approached zero gradually at low temperatures in these Co-doped Ba-materials. The coefficients along the c -axis of these Co-doped systems, however, showed rapid changes from positive values to negative values at T_c . The coefficient of $\text{Ba}(\text{Fe}_{0.926}\text{Co}_{0.074})_2\text{As}_2$ approached zero below T_c . The coefficient of $\text{Ba}(\text{Fe}_{0.92}\text{Co}_{0.08})_2\text{As}_2$, however, showed a weak temperature dependence and remained at a constant negative value at low temperatures. The coefficient along the c -axis of $\text{NdFeAsO}_{0.89}\text{F}_{0.11}$ also showed a rapid change from a positive value to a negative value at T_c . The coefficient showed a weak temperature dependence below T_c and approached zero at low temperatures. The maximum absolute value of the coefficient below T_c was about half of those for $\text{Ba}(\text{Fe}_{0.926}\text{Co}_{0.074})_2\text{As}_2$ and $\text{Ba}(\text{Fe}_{0.92}\text{Co}_{0.08})_2\text{As}_2$. Although it appears that the differences between these materials might be the result of the differences in the Einstein temperatures, a detailed analysis of the data for $\text{Ba}(\text{Fe}_{1-x}\text{Co}_x)_2\text{As}_2$ is necessary.

The magnitudes and signs of the spontaneous strains in saturation for the six superconductors are compared in Table 1 along with the symmetries of the pairing. We calculated the magnitude of $\text{NdFeAsO}_{0.89}\text{F}_{0.11}$ to be 1.3×10^{-4} at low temperature, based on the solid and broken lines in Figure 4. The linear thermal expansivities, $\Delta a/a_o$ and $\Delta c/c_o$, relative to the values of $\text{Ba}(\text{Fe}_{0.926}\text{Co}_{0.074})_2\text{As}_2$ at 1.8 K are shown in the inset of Figure 6 in ref. 30: $\Delta a/a_o$ shows almost no change at temperatures just above T_c . However, it decreases below T_c and becomes zero at low temperatures. This dependence on temperature is very similar to the temperature dependence of the lattice parameter in $\text{Ba}_{0.6}\text{K}_{0.4}\text{BiO}_3$. The change in $\text{Ba}(\text{Fe}_{0.926}\text{Co}_{0.074})_2\text{As}_2$ is -1.2×10^{-5} . The value of $\Delta c/c_o$ even changes with temperature just above T_c . To estimate the low temperature value of $\Delta c_{HT}/c_o$, the values of $\Delta c/c_o$ between T_c and 35 K were analyzed using the method discussed in

§3; the subscript HT has the same meaning as in §3. The available temperature range is so limited, however, that we could not obtain an accurate value of $\Delta c_{HT}/c_o$ at low temperatures. Finally, we estimated the value in $\text{Ba}(\text{Fe}_{0.926}\text{Co}_{0.074})_2\text{As}_2$ to be 8×10^{-5} . The maximum strain in Table 1 is widely different from the minimum one. The linear expansion of untwinned $\text{La}_{1.85}\text{Sr}_{0.15}\text{CuO}_4$ has been measured by the capacitance dilatometer under a moderate uniaxial pressure with the aim of achieving detwinning of the sample introduced by a structural phase transition at about 180 K [7]: The anomaly in α_c at T_c is approximately one tenth of our X-ray observation value [11]. Though the discrepancy might be caused by the structural phase transition, the detailed mechanism of the discrepancy is not clear. In the case of Fe-pnictide superconductors, the difference in the values obtained by the two different methods is such that one value is within twice the other value, these values seem to be reliable in Fe-pnictide superconductors.

The temperature dependence of the lattice parameter c for $\text{NdFeAsO}_{0.89}\text{F}_{0.11}$ is very similar to that for invar alloys that show low thermal expansions in their ferromagnetic phases [9]. Let us first consider the magnetovolume effect in invar alloys. Based on the Stoner theory, ferromagnetism appears when a reduction in the exchange energy of electrons exceeds the increase in their kinetic energy caused by an exchange splitting of the electron band [32]. The increase in kinetic energy is suppressed by the expansion of lattice parameters, which results in a low thermal expansion in the ferromagnetic phase. In the case of superconductors, the electronic contribution to the coefficient of volume expansion in the isotropic superconducting state, β_{es} , is obtained based on the BCS theory in the limit of weak electron-phonon coupling [6]. Using the expression, the difference between β_{es} and β_{en} , which is the electronic contribution to the coefficient of volume expansion in the normal state may be given as follows:

$$\beta_{es} - \beta_{en} = \frac{A}{\gamma} (S_{es} - C_{en}) + \frac{1}{T_c V} \left(\frac{\partial T_c}{\partial p} \right) (C_{es} - S_{es}),$$

where $\beta_{en} = AT$ and γ and p are, respectively, the coefficient of the electronic contribution to the normal-state specific heat C_{en} and the pressure. C_{es} is the electronic contribution to the superconducting-state specific heat. S_{es} and S_{en} are the entropies in the superconducting state and the normal state, respectively. Then the leading term on the right hand side of the equation is always negative, which originates from the negative dependence of Fermi energy on the volume, as in the case of invar alloys. The sign of the second term, however, is the same as the sign of $(\partial T_c / \partial p)$, which depends on the detailed mechanism of superconductivity; these terms have been observed to be both negative and positive [6]. Because the leading term vanishes at T_c , the above equation reduces to the standard Ehrenfest equation at T_c . The phenomenological approach we made in §3 is physically the same as the above analysis based on the BCS theory. However, it is not meaningful to evaluate the proportional coefficient between the spontaneous strain e and the square of the order parameter Δ^2 in

terms of the physical parameters in the above equation: The equation is appropriate under limited conditions in conventional superconductors. In addition, the coefficient is composed of two independent terms, whose numerical evaluations from the present experimental results are difficult.

5 Conclusions

The spontaneous strain generated in the Nd 1111 Fe-pnictide superconductor $\text{NdFeAsO}_{0.89}\text{F}_{0.11}$ in the superconducting phase could be explained in terms of the coupling between a superconducting order parameter and the strain. This coupling is common to various superconductors.

This work was partially supported by a Grant-in-Aid for Scientific Research from the Ministry of Education, Culture, Sports, Science and Technology. This work was also supported in part by grants from the Asahi Glass Foundation and the Hokuriku Bank. The X-ray diffractometer has been installed at the Center for Innovation in Kanazawa university.

References

1. Y. Fujii, Y. Soejima, A. Okazaki, I.K. Bdikin, G.A. Emel'chenko, A.A. Zhokhov, *Physica C* **377**, 49 (2002)
2. J.D. Jorgensen, D.G. Hinks, P.G. Radaelli, W.I.F David, R.M. Ibberson, *cond-mat/0205486* (2002)
3. D. Shoenberg, *Superconductivity*, (Cambridge University Press, Cambridge, 1962) p. 74
4. B. G. Lasarew, A. I. Suduvstov, *Doklady Akad. Nauk S.S.S.R.* **69**, 345 (1949)
5. T. H. K. Barron, G. K. White, *Heat Capacity and Thermal Expansion at Low Temperatures*, (Kluwer Academic / Plenum Publishers, New York, 1999) p. 259
6. M. A. Simpson, T. F. Smith, *J. Low Temp. Phys.* **32**, 57 (1978)
7. F. Gugenberger, C. Meingast, G. Roth, K. Grube, V. Breit, T. Weber, H. Wühl, S. Uchida, Y. Nakamura, *Phys. Rev. B* **49**, 13137 (1994)
8. T. H. K. Barron, G. K. White, *Heat Capacity and Thermal Expansion at Low Temperatures*, (Kluwer Academic / Plenum Publishers, New York, 1999) p. 200
9. M. Shiga, Y. Nakamura, *J. Phys. Soc. Jpn.* **26**, 24 (1969)
10. E.K.H. Salje, *Acta Cryst. A* **47**, (1991) 453.
11. H. Fujishita, S. Murakami, N. Nakamura, Y. Kanou, H. Okamoto, *Solid State Commun.* **145**, 246 (2008)
12. H. Fujishita, T. Yamada, H. Okamoto, S. Shitara, M. Kato, Y. Koike, *Solid State Commun.* **150**, 711 (2010)
13. Y. Kamihara, T. Watanabe, M. Hirano, H. Hosono, *J. Am. Chem. Soc.* **130**, 3296 (2008)
14. I. I. Mazin, D. J. Singh, M. D. Johannes, M. H. Du, *Phys. Rev. Lett.* **101**, 057003 (2008)
15. K. Kuroki, S. Onari, R. Arita, H. Usui, Y. Tanaka, H. Kontani, H. Aoki, *Phys. Rev. Lett.* **101**, 087004 (2008)
16. M. Sato, Y. Kobayashi, S.C. Lee, H. Takahashi, E. Satomi, Y. Miura, *J. Phys. Soc. Jpn.* **79**, 014710 (2010)
17. S. C. Lee, E. Satomi, Y. Kobayashi, M. Sato, *J. Phys. Soc. Jpn.* **79**, 023702 (2010)
18. S. Onari, H. Kontani, M. Sato, *Phys. Rev. B* **81**, 060504 (2010)
19. A. Kawabata, S. C. Lee, T. Moyoshi, Y. Kobayashi, M. Sato, *J. Phys. Soc. Jpn.* **77**, 103704 (2008)
20. A. Kawabata, S. C. Lee, T. Moyoshi, Y. Kobayashi, M. Sato, *Proc. Int. Symp. Fe-Pnictide Superconductors*, *J. Phys. Soc. Jpn.* **77**, Suppl. C, 147 (2008)
21. H. Toraya, *J. Appl. Cryst.* **19**, 440 (1986)
22. H. Toraya, *Adv. X-ray Anal.* **37**, 37 (1994)
23. Y. Qiu, Wei Bao, Q. Huang, T. Yildirim, J. M. Simmons, M. A. Green, J. W. Lynn, Y. C. Gasparovic, J. Li, T. Wu, G. Wu, X. H. Chen, *Phys. Rev. Lett.* **101**, 257002 (2008)
24. E.K.H. Salje, *Phase Transitions in Ferroelectric and Elastic Crystals*, student edn. (Cambridge University Press, Cambridge, 1993) p.22
25. M. Calamitoutou, I. Margiolaki, A. Gantis, E. Siranidi, Z. A. Ren, Z. X. Zhao, *EPL* **91**, 57005 (2010)
26. B. Mühlischlegel, *Z. Physik* **155**, 313 (1959)
27. S. Tsuda, T. Yokoya, Y. Takano, H. Kito, A. Matsushita, F. Yin, J. Itoh, H. Harima, S. Shin, *Phys. Rev. Lett.* **91**, 127001 (2003)
28. N. Ni, M. E. Tillman, J.-Q. Yan, A. Kracher, S. T. Hannahs, S. L. Bud'ko, P. C. Canfield, *Phys. Rev. B* **78**, 214515 (2008)
29. J.H. Chu, J. G. Analytis, C. Kucharczyk, I. R. Fisher, *Phys. Rev. B* **79**, 014506 (2009)
30. S. L. Bud'ko, N. Ni, S. Nandi, G. M. Schmiedeshoff, P. C. Canfield, *Phys. Rev. B* **79**, 054525 (2009)
31. F. Hardy, P. Adelmann, T. Wolf, H. v. Lohneysen, C. Meingast, *Phys. Rev. Lett.* **102**, 187004 (2009)
32. H. Ibach, H. Lüth, *Solid-State Physics, An Introduction to Principles of Material Science*, fourth edn. (Springer, Berlin, 2009) p. 201

Table 1. Comparison of spontaneous strains in saturation of six superconductors and pairing symmetries of their superconductivities. The directions of the spontaneous strains are indicated in parentheses.

superconductor	spontaneous strain in saturation		reference	symmetry of superconductivity
$\text{La}_{1.85}\text{Sr}_{0.15}\text{CuO}_4$	$0.53 \times 10^{-5}(\text{c})$		[7] ¹	d-wave
	$7.0 \times 10^{-5}(\text{c})$		[11]	
$\text{YBa}_2\text{Cu}_3\text{O}_{6.5}$	$2.4 \times 10^{-5}(\text{a})$		[1, 12]	d-wave
$\text{Ba}_{0.6}\text{K}_{0.4}\text{BiO}_3$	$-5.1 \times 10^{-5}(\text{a})$		[12]	typical s-wave
MgB_2	$1.4 \times 10^{-5}(\text{a})$	$1.0 \times 10^{-5}(\text{c})$	[2, 11]	two-band s-wave
$\text{NdFeAsO}_{0.89}\text{F}_{0.11}$	$13 \times 10^{-5}(\text{c})$		this work	five-band s-wave
$\text{Ba}(\text{Fe}_{0.926}\text{Co}_{0.074})_2\text{As}_2$	$8 \times 10^{-5}(\text{c})$	$-1.2 \times 10^{-5}(\text{a})$	[30] ²	five-band s-wave

¹ This value was obtained by the integration of $\alpha^* = \alpha - \alpha_{\text{spine}}$ below $\alpha^*(T_c)$ between 10 K and T_c in Figure 4 in ref. 7.² These values were obtained by the analyses of the linear thermal expansivities relative to the values at 1.8K given in ref. 30 (see text).